Civil Engineering Dimension
https://ced.petra.ac.id

Impact of Anchor Drag on Subsea Pipeline Integrity: Numerical Study on Crack Propagation and Leakage

Arianta[1], Tawekal, R.L.[2,3]*, Santoso, J.F.[2], and Ilman, E.C.[2,3]
[1] Civil Engineering Program, Universitas Pertamina, INDONESIA
[2] Ocean Engineering Program, Institut Teknologi Bandung, INDONESIA
[3] Offshore Engineering Research Group, Institut Teknologi Bandung, INDONESIA

DOI: https://doi.org/10.9744/ced.28.1.1-10

Article Info:
Submitted: Jan 14, 2025
Reviewed: Feb 18, 2025
Accepted: Dec 09, 2025

Keywords:
crack propagation,
XFEM,
offshore pipeline,
finite element,
anchor drag.

Corresponding Author:
Tawekal, R.L.
Ocean Engineering Program,
Institut Teknologi Bandung,
INDONESIA
Email: ricky@ocean.itb.ac.id

Abstract

Anchor drag incidents impacting subsea pipelines lead to structural failure, driven primarily by crack propagation under mechanical stress. This study employs finite element modelling (FEM) and the extended finite element method (XFEM) to evaluate how initial crack dimensions (depth: 4–6 mm; length: 20–60 mm) affect pipeline integrity. Results indicate that pipelines with smaller initial cracks (4 mm depth) resist leakage until an anchor drag distance of 67.839 m, whereas larger cracks (6 mm depth) fail at 33.389 m, emphasizing crack depth as the critical factor in reducing structural resilience. Crack propagation follows a triphasic pattern: slow initiation, rapid acceleration at 25–35 m drag distance, and deceleration near the pipe wall. Larger cracks propagate faster, with 6 mm depth cracks reaching critical failure earlier than smaller defects.

INTRODUCTION

Subsea pipelines are an efficient and economical means of transporting hydrocarbon products between offshore and land facilities for export. To ensure the safe and optimal design of these pipelines, strict safety standards and regulations are in place to mitigate potential failure modes resulting from operation-based design. However, pipelines remain vulnerable to external damage. One of the leading causes of pipeline accidents is ship anchoring, which, although rare, can result in catastrophic damage. According to historical data from PARLOC 2001 [1], anchor-related failure contributed to 21% of subsea pipeline incidents, ranking as the third most prevalent after impact (mechanical damage) and corrosion. A notable example occurred in 2018 when a subsea oil pipeline in Balikpapan Bay, Indonesia, failed due to anchor drag. Situated 20 m below the sea surface, the pipeline dragged over 100 m, resulting in significant environmental and economic consequences. Additionally, four other cases of anchor-dragging pipelines were reported between 1987 and 2011 [2]. Bartolini et al. [3] expanded this understanding by investigating critical parameters influencing ship anchor impacts during drag events. These include anchor size (determining its capacity to interact with the pipeline), drag velocity, anchor incidence angle, anchor chain configuration (accounting for chain length and water depth), and seabed soil properties.

Mustafina [4] investigated the interaction between anchors of varying sizes and subsea pipelines, employing analytical, experimental, and global-scale modelling approaches for 40-inch and 16-inch diameter pipelines in the North Sea. The study demonstrated that not all anchor systems are capable of damaging pipelines. For an anchor to pose a risk, its size must be sufficient to hook the pipeline and exert sufficient force to drag it. Furthermore, the anchor system must reach the seabed to engage with the pipeline, a process critically dependent on chain length, vessel speed, and anchor dimensions. Building on Mustafina's criteria, Tawekal et al. [5] expanded this research by conducting a comprehensive stress analysis of a subsea pipeline system in the Madura Strait. Their work focused on

Note : Discussion is expected before July, 1st 2026, and will be published in the "Civil Engineering Dimension", volume 28, number 2, September 2026.
ISSN : 1410-9530 print / 1979-570X online
Published by : **Petra Christian University**

the three largest vessels whose routes crossed the pipeline's path. Global analysis identified maximum displacement conditions, while local stress analyses evaluated indentation depth, stress, and strain levels under these scenarios. These findings underscore the critical need to investigate crack behaviour under anchor-induced stresses, particularly how defects influence structural failure. To evaluate material toughness in the presence of crack defects, the stress intensity factor (SIF) at the crack tip is compared to the material's fracture toughness. The SIF quantifies the elastic stress field near the crack tip, governing stress distribution in the surrounding material [6]. Its magnitude depends on structural geometry, crack characteristics, and applied load magnitude.

To address this gap, modelling becomes essential when assessing the impact of defects on material strength. The finite element method (FEM), a widely used numerical technique for solving differential equations, struggles with computational efficiency when modelling large discontinuities like cracks due to the high mesh resolution required for convergence [7]. To overcome this limitation, Belytschko et al. introduced the extended finite element method (XFEM) [8], which eliminates the need for mesh alignment with discontinuities and avoids remeshing during crack propagation [9]. XFEM enriches the finite element mesh with a discontinuity function (jump function) and a near-tip asymptotic function [10], enabling crack modelling without predefined geometry. A conventional mesh without incorporating crack geometry; subsequently, additional degrees of freedom are assigned to nodes along crack paths or near crack tips [11], making XFEM uniquely suited for dynamic fracture analysis.

Using the advanced capabilities of the XFEM, this study investigates ship anchor-pipeline interaction through finite element modelling. The analysis assumes an initial circumferential crack at the 9 o'clock position on the pipe profile, with depths of 4, 5, and 6 mm and lengths of 20, 40, and 60 mm. XFEM is employed to simulate crack propagation under anchor drag conditions, enabling the evaluation of crack growth behaviour under varying load scenarios. The primary objective is to quantify the influence of initial crack dimensions on pipeline failure thresholds, providing insights into how crack depth and length affect the maximum allowable anchor drag distance before leakage occurs.

CASE STUDY

Anchor-Pipeline Interaction

As defined in DNV-RP-F107 [12], two primary scenarios govern anchor-pipeline interactions: anchor drop, where a falling anchor generates localized impact loads, and anchor drag, where a hooked anchor exerts initial impact loads during contact, followed by sustained pullover loads post-hooking. While DNV-RP-F107 outlines these failure modes, it does not provide explicit equations for quantifying anchor-induced dynamic forces, revealing a critical gap in standardized load quantification methodologies. To address this limitation, this study employs the FEM in Abaqus to analyze anchor impact effects on a 254 mm (10 inch) diameter API PSL2 steel pipeline with a 12.7 mm (0.5 inch) wall thickness. The initial model, illustrated in Figure 1, involved modelling a 5 km long pipe using beam elements (PIPE31 Abaqus code), with the seabed laydowns were represented as rigid planes. The pipeline was geometrically parameterized as a 5,000 m straight wire atop a rigid seabed domain (5,000 m × 1,500 m), discretized into 50,000 pipe elements (100 mm each). Due to the absence of experimental stress-strain data, the Ramberg-Osgood model generated an engineering stress-strain curve, later converted to a true stress-strain relationship to account for plastic deformation effects.

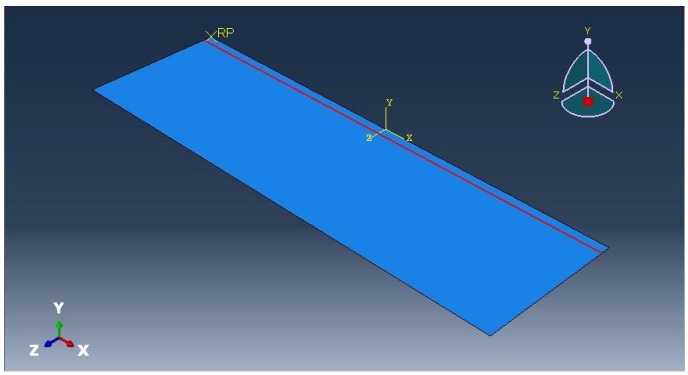

Figure 1. Initial Model Anchor Pipeline Interaction

Sequential analysis steps are static analysis, operational loading, and anchor force imposition, which were implemented to simulate transient loads. Tangential contact mechanics governed pipeline-seabed interactions, with a

friction coefficient of 0.3 between the seabed (master surface) and pipeline (slave surface). Boundary conditions permit free axial displacement at pipeline ends while constraining seabed movement. The maximum drag force during pullover was calculated using the DNV-RP-F111 [13] using the equation below, enabling parametric evaluation across pipe diameters from 254 mm (10 inches) to 1,016 mm (40 inches).

$$F_p = C_F\, V\sqrt{m_t k_w} \tag{1}$$

$$C_F = 8\left(1 - e^{-0.8\bar{H}}\right) \tag{2}$$

$$\bar{H} = \frac{H_{sp}+OD/2+0.2}{B_t} \tag{3}$$

$$k_w = \frac{3.5\times10^7}{L_w} \tag{4}$$

Where F_p is the pullover horizontal maximum force, C_F is the empirical geometry coefficient of pipe and trawl board interaction, V is the speed of pull-over, m_t is the trawl board mass, k_w is the warp line stiffness, $\bar{H}$ is the non-dimensional height, and H_{SP} is the pipeline free span height. The initial model utilizes displacement values derived from the anchor's maximum tensile force as input for simulating anchor movement in the second model.

The second model builds upon the displacement data from the initial model's anchor tensile force analysis to simulate anchor-pipeline interaction. It incorporates a stockless anchor modelled as a rigid shell element with a 300 mm width and 40° inclination, compliant with DNVGL-RU-SHIP-Pt3Ch11 [14]. The pipeline system consists of two 2,500 m wire-type segments connected by a 3 m solid section, explicitly modelled with outer diameter and thickness parameters to serve as the anchor pull zone. The seabed is divided into two 3,000 m × 1,000 m rigid sections, ensuring spatial separation for deformation analysis.

Mesh configuration is meticulously implemented, with the wire-type pipeline segments discretized into 2,500 linear elements (1 m per element) and the solid pipe section refined to a uniform 10 mm mesh. The anchor and seabed are modelled as rigid bodies to prioritize computational efficiency. During assembly, the anchor is positioned 0.75 m behind the solid pipe, while the pipelines are offset 1 m from the seabed edges to replicate realistic deployment geometry.

Kinematic coupling constraints enforce displacement compatibility between the solid pipe section and adjacent wire segments, while rigid body constraints applied to the seabed and anchor isolate deformation analysis exclusively to the pipeline system. Advanced modelling techniques, as illustrated in Figure 2, utilize solid elements to represent pipe segments subjected to crushing forces from the anchor, with beam elements connecting these segments to maintain structural continuity.

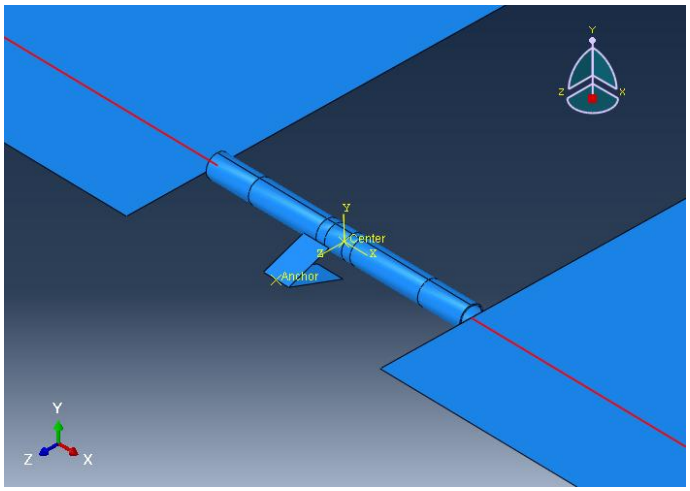

Figure 2. Second Model of Anchor Pipeline Interaction

Crack Analysis with XFEM

The crack is modeled as an internal discontinuity within the elements, enabling the analysis of crack initiation and growth without altering the mesh. Levén & Rickert offer guidance on meshing techniques to achieve stress intensity

factor values close to theoretical predictions [15]. The pipe crack modelling is a submodel of Figure 2 and uses finer mesh elements, as shown in Figure 4. The number of solid elements (C3D8R Abaqus code) ranged from 15,800 to 16,100 elements in the study by Santoso et al [16]. Table 1 outlines the case scenario of crack dimensions with an external circumferential semi-elliptical crack shape. The crack position is assumed to be at maximum stress when the anchor strikes the pipe, as depicted in Figure 3.

Table 1. Initial Crack Dimensions

Case	Initial Crack Depth (a) (mm)	Circumferential Crack Length (2c) (mm)
1	4	20
2	4	40
3	4	60
4	5	20
5	5	40
6	5	60
7	6	20
8	6	40
9	6	60

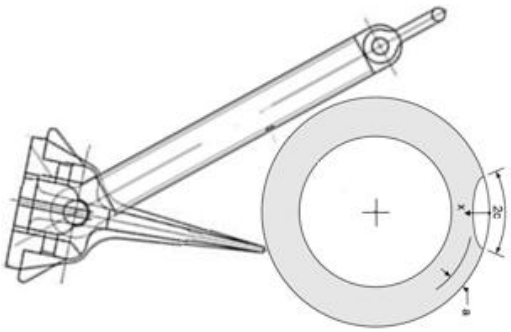

Figure 3. Initial Crack Location

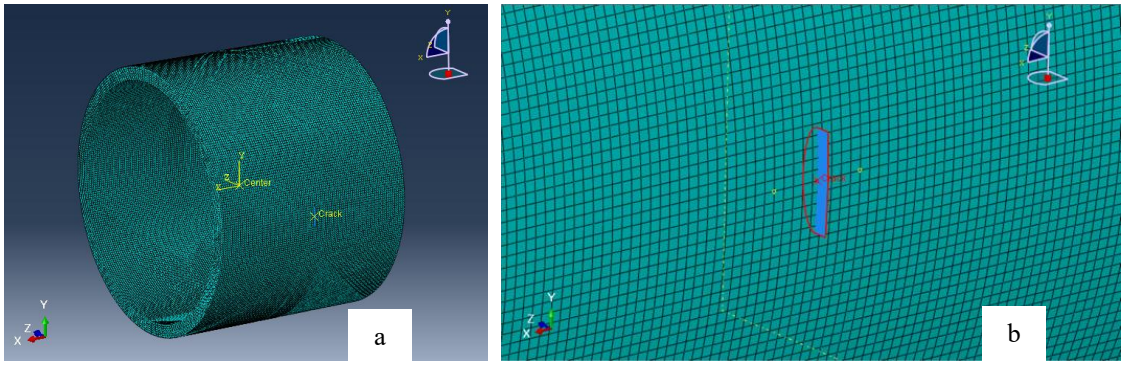

Figure 4. (a) Pipeline Sub-model from the Second Model, (b) Initial Crack Position

RESULTS AND DISCUSSION

The analysis of ship anchor-subsea pipeline interaction under a maximum tensile force of 578.81 kN revealed that the pipeline could withstand anchor drag distances of up to 214.565 m, resulting in a total displaced length of 2.757 km (Figure 5).

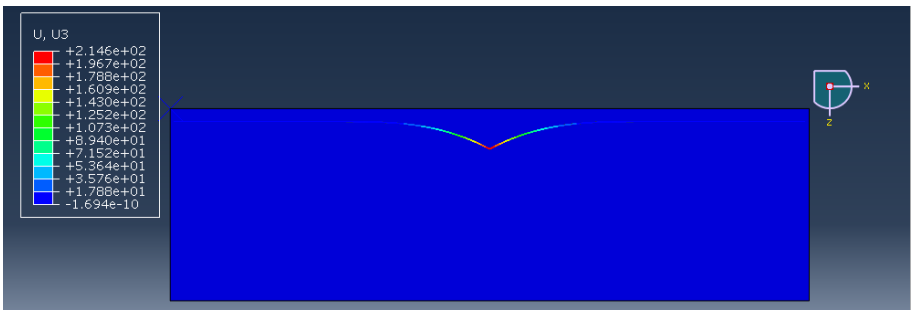

Figure 5. Maximum Displacement of Pipeline due to Anchor Drag

Using beam elements, the Abaqus simulation generated a pipe profile section point (SP), visualized in Figure 6. Stress mapping at the SP (Figure 7) identified significant stress concentrations at SP 3 and SP 7, where the pipeline reached its material yield limit during maximum displacement, consistent with Tawekal et al. [5]. Elevated stress concentrations occurred at both the anchor contact point and the opposite side of the pipeline, confirming the likelihood of crack initiation and propagation at SP 7 under high-stress conditions.

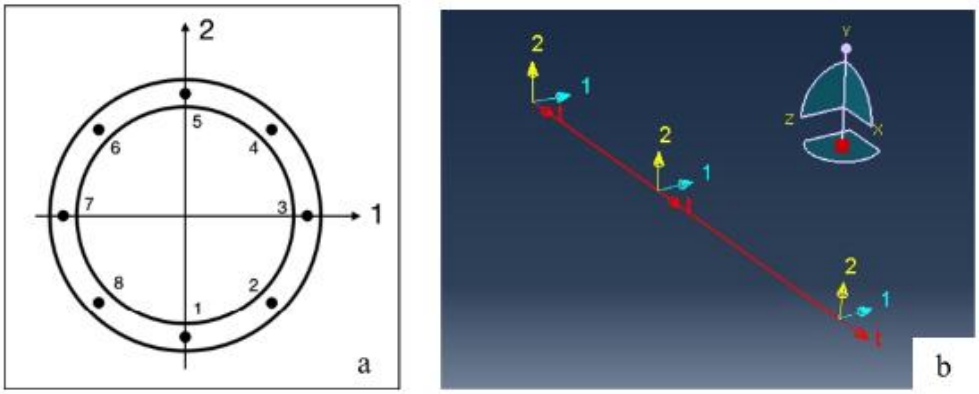

Figure 6. (a) Cylinder Section Point, (b) Local Coordinate of Beam Element with Pipe Profile

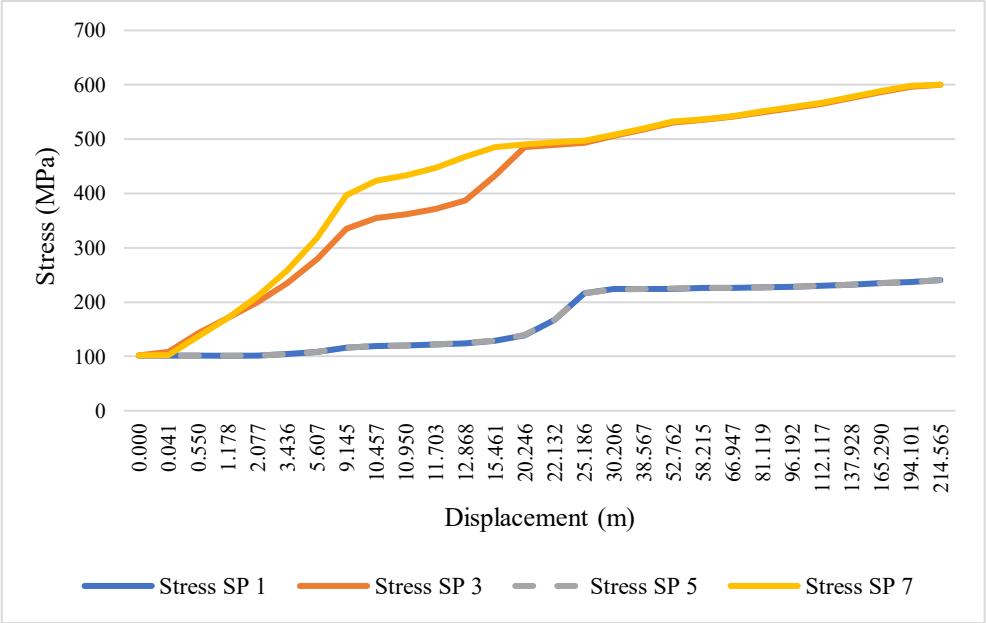

Figure 7. Pipeline Stress at SP due to Anchor Drag

Displacement data from the anchor-pipeline interaction served as input for crack analysis using solid elements. Results showed that SIF values exceeded the pipeline material's fracture toughness in all crack dimension cases (Figure 8), indicating inevitable crack propagation under applied loads. Crack initiation was determined by monitoring the STATUSXFEM parameter in Abaqus, where:

- STATUSXFEM = 1: Fully cracked element.
- 0 < STATUSXFEM < 1: Partially cracked element.
- STATUSXFEM = 0: Intact element.

By tracking elements with STATUSXFEM > 0 during incremental crack propagation, the timing of crack initiation could be estimated. This approach enabled precise identification of crack onset and progression. Figure 9 illustrates the monitoring process of STATUSXFEM, where color variations in the elements depict crack propagation at each increment until the anchor ceases to drag the pipeline.

Figure 10 demonstrates that larger crack dimensions (depth and length) accelerate propagation rates, correlating with higher SIF values (Figure 8). Cracks at depths of 5 mm and 6 mm exhibited minimal differences in pull distance (25–26 m), suggesting reduced sensitivity to depth increases beyond 5 mm. Detailed crack growth analysis (Figures 11–13) further revealed accelerated propagation for larger cracks.

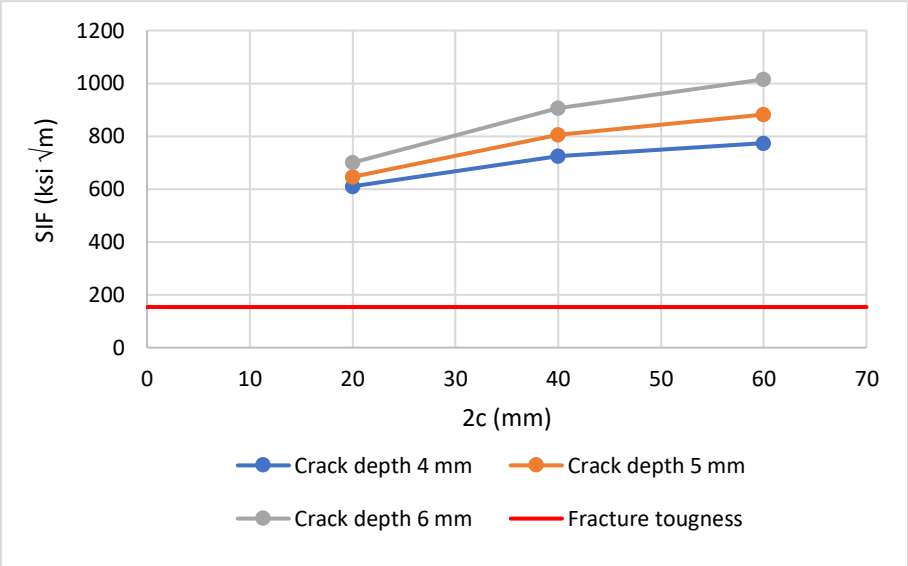

Figure 8. SIF for all Cases

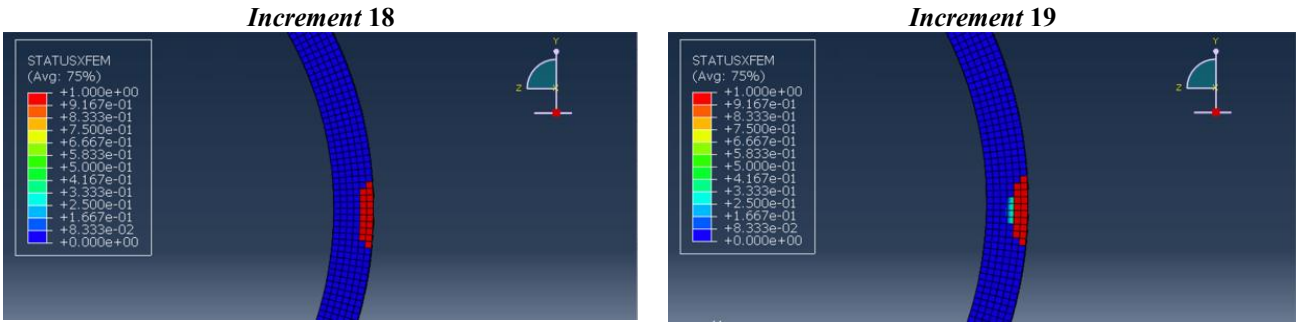

Figure 9. STATUSXFEM

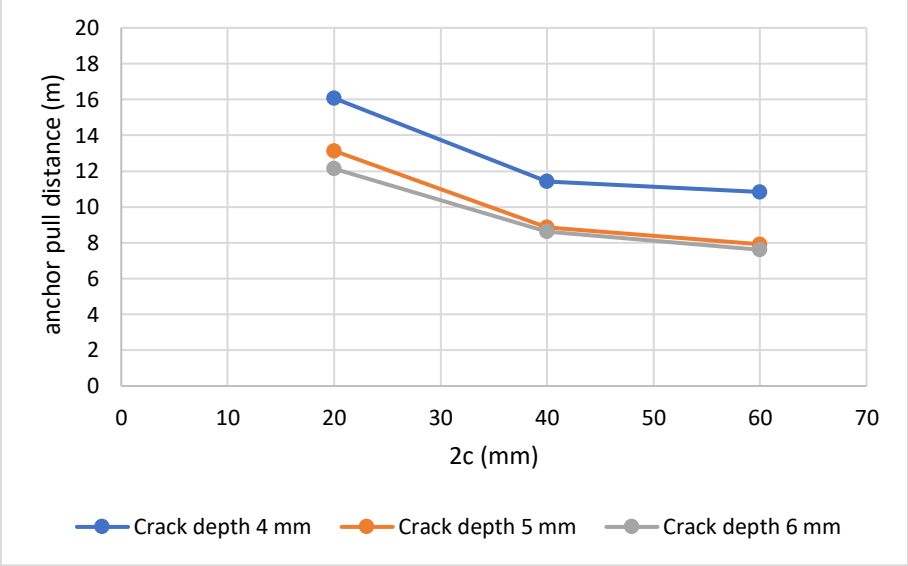

Figure 10. Initial Crack Propagation according to Anchor Pull Distance

The analysis of Figures 11–13 reveals that crack propagation progresses through three distinct phases: an initial period of slow growth, followed by rapid acceleration at pull distances of 25–35 m, and eventual deceleration as cracks approach the pipe wall thickness. This pattern is consistent across all cases. Notably, the minimal discrepancy in propagation rates between 5 mm and 6 mm crack depths, evident in their identical pull distances of 25–26 m is attributed to the use of identical mesh configurations for both cases. To enhance accuracy, refining the mesh density at crack tips, akin to the methodology applied in stress intensity factor (SIF) calculations, could ensure distinct element rows for crack tips, thereby better capturing depth-specific propagation behaviours.

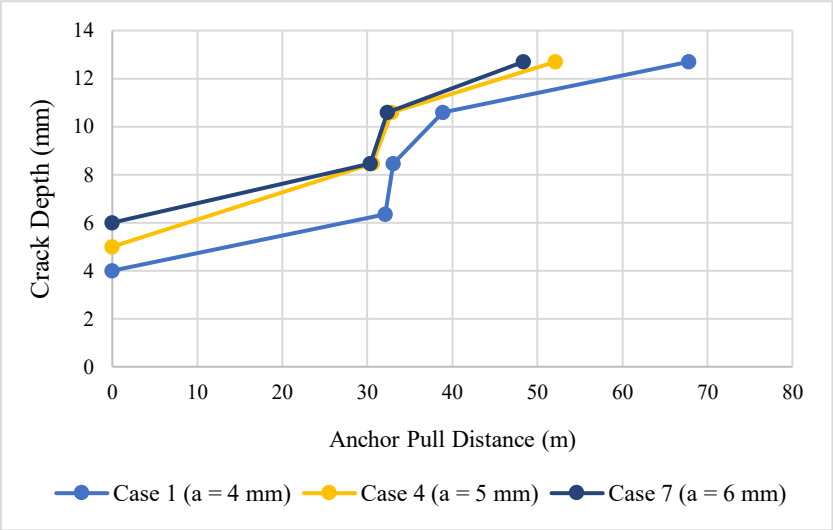

Figure 11. Crack Depth Growth with Initial Circumferential Crack Length 20 mm

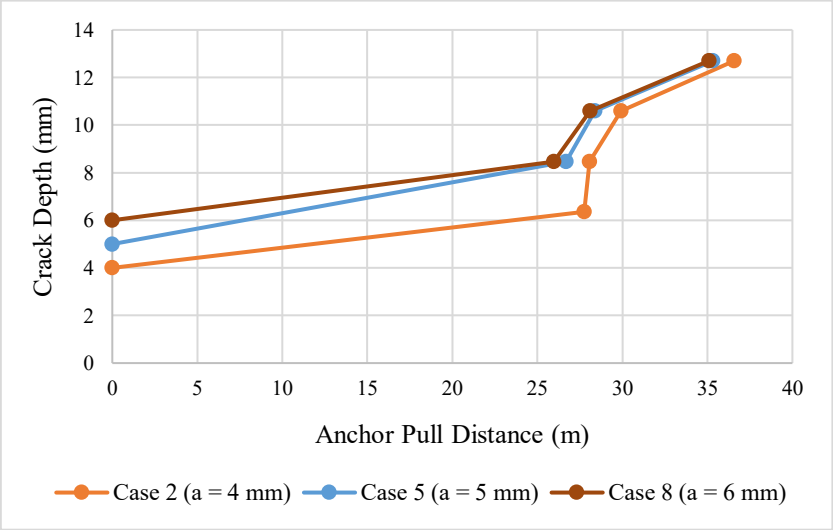

Figure 12. Crack Depth Growth with Initial Circumferential Crack Length 40 mm

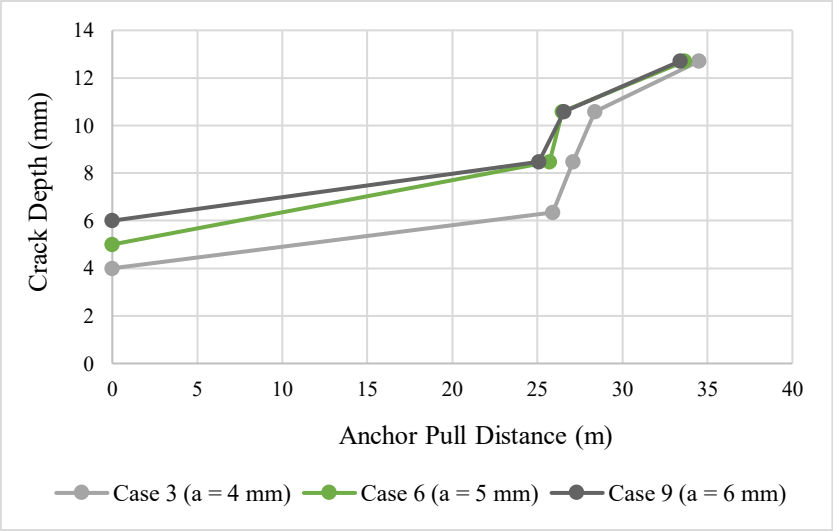

Figure 13. Crack Depth Growth with Initial Circumferential Crack Length 60 mm

Figure 14 compares stress concentrations across cases with varying crack depths but identical lengths. The negligible difference between 5 mm and 6 mm depths resulted in similar propagation rates during anchor pull. However, the 6 mm crack-initiated propagation marginally earlier, underscoring the critical role of initial crack size in structural failure.

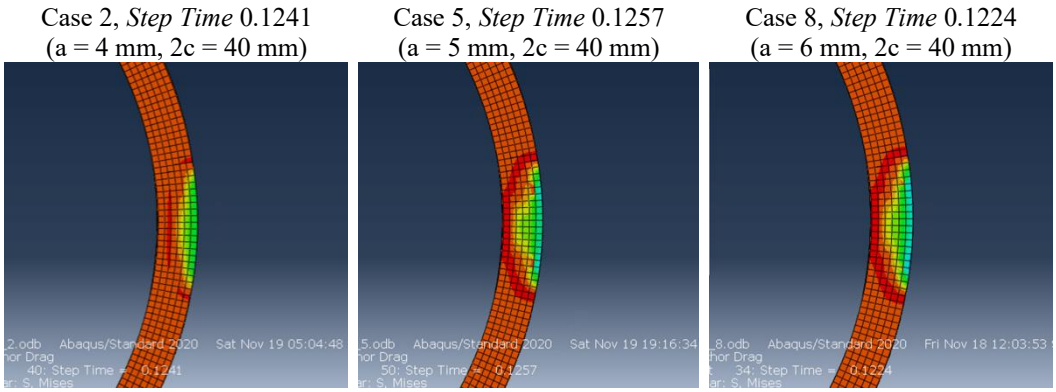

Figure 14. Comparison Stress Concentrations at the Crack Tip

When examining the maximum anchor pull distance (R_{max}) that leads to crack propagation and subsequent pipe leakage, it is evident that larger initial crack dimensions lead to earlier leakage compared to smaller crack dimensions. The pipe can withstand pulling up to 67.839 m before leaking for the smallest crack variation. In contrast, the pipe only needs to be pulled 33.389 m to experience leakage for the largest crack variation, see Figure 15. This significant difference underscores the critical impact of initial crack size on the structural integrity of the pipeline under anchor pull stress. To more clearly see the impact of crack dimension parameters on pipeline leakage, a graph was created showing the distance an anchor can be pulled until the pipeline leaks, based on the initial crack depth and initial crack length. It can be observed that the maximum distance an anchor can be pulled, which the pipeline can withstand, tends to decrease as the initial crack depth and length increase.

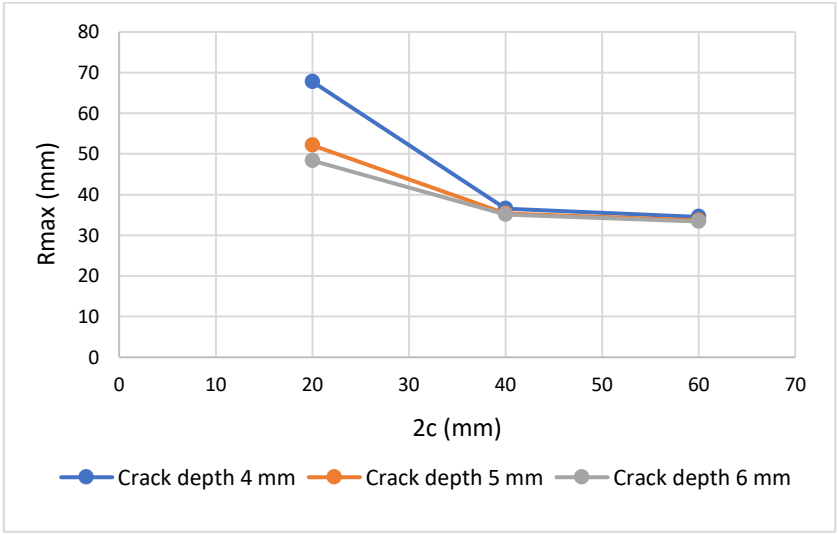

Figure 15. Anchor Pull Distance to Pipeline Leakage

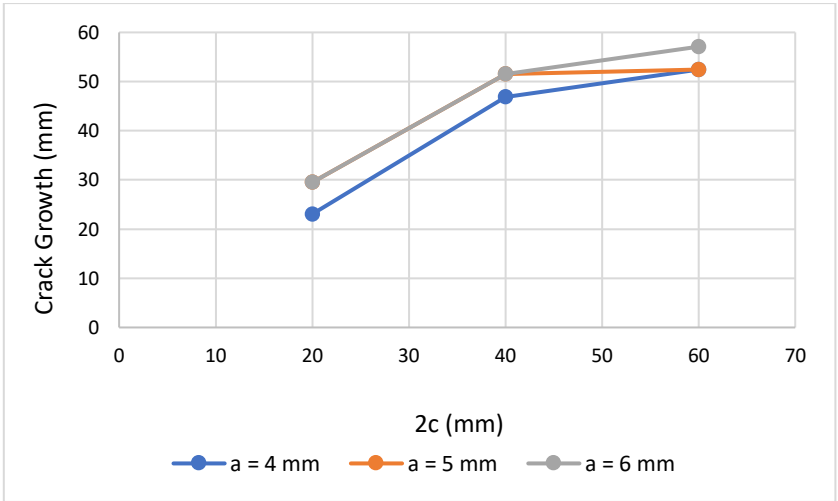

Figure 16. Crack Growth

Furthermore, Figure 16 demonstrates that cracks with larger initial lengths produce longer final crack lengths and greater crack growth. The figure summarizes final crack measurements across all initial crack cases, revealing minimal variation in total crack growth for cases with similar initial dimensions. Specifically, crack length growth on the pipeline's outer surface yielded identical values in several cases, suggesting that minor differences in initial crack dimensions do not significantly influence overall propagation behaviour.

CONCLUSIONS

The study demonstrates that the size of initial cracks in pipelines significantly affects pipeline integrity. It is evident that pipelines with smaller initial cracks, with a depth of 4 mm, can withstand anchor drag up to 67.839 m before leaking. In contrast, a larger initial crack, with a depth of 6 mm, leads to leakage at a significantly shorter distance, at 33.389 m. Crack depth has a more pronounced impact on the maximum drag distance before leakage occurs compared to crack length.

SIF analysis further reveals that deeper cracks generate higher SIF values, correlating with elevated stress concentrations at the crack tip. Notably, cracks with depths of 5 mm and 6 mm exhibit identical SIF values, both exceeding those of 4 mm-depth cracks, which indicates a marked increase in failure vulnerability as crack depth increases. Crack propagation progresses through three distinct phases: an initial period of slow growth, followed by rapid acceleration at pull distances of 25–35 m, and eventual deceleration as cracks approach the pipe wall thickness. Larger cracks propagate more rapidly, with 6 mm-depth cracks reaching critical failure thresholds faster than their 4 mm counterparts. These findings emphasize the necessity of rigorous monitoring and mitigation of initial crack dimensions, particularly depth, to ensure pipeline safety under external mechanical stresses.

REFERENCES

1. Liu, H.B. and Zhao, X.L., Fatigue of Subsea Pipelines under Combined Actions, *Journal of the Construction Division*, ASCE, 23(1), 2013.
2. Mulyadi, S., Kobayashi, E., Wakabayashi, N., Pitana, T., Citrosiswoyo, W., and Prasetyo, E., Estimation Method for Dragged Anchor Accident Frequency on Subsea Pipelines in Busy Port Areas, *Journal of the Japan Society of Naval Architects and Ocean Engineers*, 20(173), 2015, pp. 173–183.
3. Bartolini, L., Marchionni, L., Parrella, A., and Vitali, L., Advanced FE Modelling Approach for Pipeline Hooking Interaction of Dragged Anchors, *Proceedings of the ASME 2018 37th International Conference on Ocean, Offshore and Arctic Engineering*, Madrid, Spain, June 17–22, 2018.
4. Mustafina, A.F., *Anchor Damage Assessment of Subsea Pipelines - Optimization of Design Methodology*, Master's Thesis, University of Stavanger, 2015.
5. Tawekal, R.L., Allo, R.P.R., and Taufik, A., Damage Analysis of Subsea Pipeline due to Anchor Drag, *International Journal of Applied Engineering Research*, 12(15), 2017, pp. 5016–5021.
6. Anderson, T.L., *Fracture Mechanics: Fundamentals and Applications*, Fourth edition, CRC Press, 2017.
7. Khoei, A.R., *Extended Finite Element Method: Theory and Applications*, John Wiley & Sons, 2015.
8. Belytschko, T. and Black, T., Elastic Crack Growth in Finite Elements with Minimal Remeshing, *International Journal for Numerical Methods in Engineering*, 45(5), 1999, pp. 601–620.
9. Arianta, Tawekal, R.L., Taufik, A., and Rildova, Determination of Geometry Factor of Crack in Dented API 5L X65 Pipeline using Finite Element Method, *International Journal of Scientific & Engineering Research*, 5(9), 2016.
10. Shi, J., Chopp, D., Lua, J., Sukumar, N., and Belytschko, T., Abaqus Implementation of Extended Finite Element Method using a Level Set Representation for Three-Dimensional Fatigue Crack Growth and Life Predictions, *Engineering Fracture Mechanics*, 77(14), 2010, pp. 2840–2863.
11. Valadi, Z., Bayesteh, H., and Mohammadi, S., XFEM Fracture Analysis of Cracked Pipeline with and without FRP Composite Repairs, *Mechanics of Advanced Materials and Structures*, 27(22), 2018, pp. 1888–1899.
12. Det Norske Veritas, *Risk Assessment of Pipeline Protection (DNV-RP-F107)*, 2010.
13. Det Norske Veritas, *Interference Between Trawl Gear and Pipelines (DNV-RP-F111)*, 2010.
14. Det Norske Veritas, *Hull Equipment, Supporting Structure and Appendages (DNVGL-RU-SHIP-Pt3Ch11)*, 2017.
15. Levén, M. and Rickert, D., *Stationary 3D Crack Analysis with Abaqus XFEM for Integrity Assessment of Subsea Equipment,* Master's Thesis, Chalmers University of Technology, 2012.

16. Santoso, J.F., Tawekal, R.L., Arianta, and Ilman, E.C., Numerical Assessment of Subsea Pipeline Pressure Capacity due to External Circumferential Semi-Elliptical Crack, *International Journal of Geomate*, 25(108), 2023, pp. 138–145.